Influence of different mechanisms on the constitutive behaviour of textile reinforced concrete*

Jens Hartig[1], Frank Jesse[2], Ulrich Häußler-Combe[3]

Summary: Textile Reinforced Concrete shows a complex load-bearing behaviour, which depends on material properties of the composite constituents and load transfer mechanisms in between. These properties cannot be modified arbitrarily in experimental investigations, which complicates identification of the impact of certain mechanisms on composite's behaviour. In this respect, theoretical investigations offer the possibility to study the influence of individual parameters. At first, experimental results of tensile-loaded specimens are given, which help to identify different mechanisms in advance. Afterwards, respective results of numerical calculations with a reduced two-dimensional model are presented to study these mechanisms, including the effects of a reduced stiffness in the cracked state, yarn waviness and tension softening of the cementitious matrix.

1 Introduction

For textile reinforced concrete (TRC), multi-filament yarns of high-performance fibres, e. g. carbon or alkali-resistant (AR) glass, are used as reinforcement. These fibre materials provide high tensile strengths and Young's moduli as well as good durability if exposed to the alkaline environment of concrete. The composition of the yarns of a vast number of filaments and the high viscosity of the cement matrix lead to an incomplete and inhomogeneous penetration of the yarns with matrix, and thus to different bond conditions in the inner and outer zones of a yarn, which gives rise to the complex material behaviour of TRC.

A number of effects influence the constitutive behaviour of TRC, most often in combination, which complicates the clear identification of the extent of influence. In experimental investigations, isolated observation of single effects is difficult since the material properties cannot be modified arbitrarily. On the other hand, theoretical investigations provide this ability, but the respective models have to be in conformance with reality, i. e. with experiments.

*This is a peer-reviewed paper. Online available: urn:nbn:de:bsz:14-ds-1244044908960-34481
[1]Dipl.-Ing., Institute of Concrete Structures, Technische Universität Dresden
[2]Dr.-Ing., Institute of Concrete Structures, Technische Universität Dresden
[3]Prof. Dr.-Ing. habil., Institute of Concrete Structures, Technische Universität Dresden

Investigations in this paper are limited to the case of tensile loading with multiple matrix cracking. Respective experiments were performed e. g. by [13] and [10]. In the following, only selected results corresponding to investigations of [10] shall be regarded. Theoretical investigations concerning the uniaxial tensile behaviour of TRC were performed with different approaches, e. g. an analytical model by [15], a semi-analytical model by [11] and numerical models, e. g. by [3] and [7], while the last is used for the numerical investigations in this paper.

2 Experimental setup and general structural behaviour

In order to study the uniaxial tensile behaviour of TRC with multiple cracking, tensile specimens with reinforcement ratios ranging from approx. 1 % up to 3 % and dimensions of 500 mm × 100 mm × 8 mm (length × width × height) were used in [10] (see also for matrix composition). Displacement controlled tests were carried out in a standard hydraulic testing machine where the load was transferred to the specimen by means of clamping. The structural response is given as mean stress-mean strain relations, where the mean stress is calculated from the measured force and the cross-sectional area of the matrix. The mean strain is derived from deformation measurements using a clip-on extensometer of 200 mm length.

In Figure 1, results of specimens reinforced with biaxial double tricot-bonded fabrics (7.2 mm yarn spacing in both directions) of AR-glass yarns (Vetrotex 1200 tex) with and without additional polymer-coating are shown. Although the fibres used as reinforcement are identical in both directions, the warp direction shows macroscopic waviness due to the production process, which is not the case to the same extent in the weft direction. As it can be seen in Figure 1, the stress-strain relations can be subdivided into three main states. Firstly, the uncracked state where the matrix bears almost the whole load followed by multiple cracking, which requires a sufficient amount of reinforcement to bridge the cracks. This state is associated with a reduced mean stiffness compared to the uncracked state. The final crack pattern is reached at lower strain levels for higher reinforcement ratios compared to lower reinforcement ratios. Additionally, the post-cracking resistance of the matrix, also called tension softening, might lead to a reduced strain at the end of the cracking state and a smoother transition to the final cracking state, which can be seen in Figure 1 especially for the cases of higher reinforcement ratios and loading in weft direction of the reinforcement.

In the final cracking state, the slopes of the stress-strain relations increase again. This is dominated by the stiffness of the reinforcement, which carries most of the load in the cracked part of the specimen. However between the cracks, the matrix participates in load-bearing leading to the well-known tension stiffening effect. This effect might be masked by a delayed loading of the reinforcement due to an initial waviness of the filaments, which could lead to „negative“ tension stiffening. This is observable in Figure 1, if the stress-strain relations for the loading in weft and warp direction of the fabric are compared. The warp direction is less stretched in the production process and shows initial waviness, which leads to larger deformations in case of matrix cracking and thus to a larger strain range of the cracking state as well as a stress-strain response shifted to larger strains in the final cracking state.

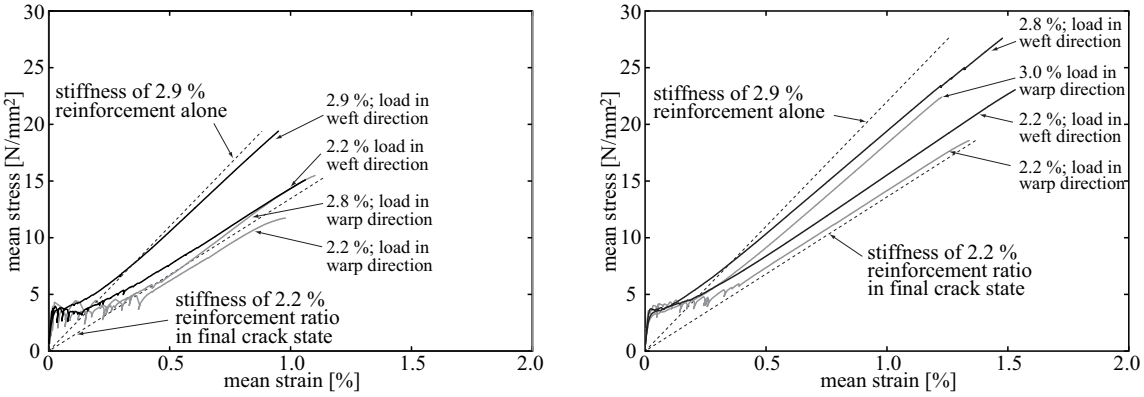

(a) Uncoated fabrics

(b) Fabrics with polymer-coating based on Styrol-Butadien

Figure 1: Experimental stress-strain relations with different reinforcement ratios, coatings and fabric orientations

Regarding the slope of the stress-strain relation in the post-cracking state, it is observable that the mean stiffness of the specimens is lower than the stiffness of the reinforcement itself, independent of coating and fabric orientation. As pointed out by [10], the reason is that a part of the reinforcement does not participate in load bearing. One possible explanation is given in [10] by a premature failure of filaments in the fill-in zone during concrete cracking. However, this explanation contradicts with the fact that for increasing reinforcement ratios the stress in the reinforcement during cracking decreases and might not reach the filament tensile strength. Additionally, the post-cracking resistance of the matrix reduces the stress in the reinforcement fibres right after matrix cracking. Thus, the assumption of simultaneous matrix cracking and filament failure in the fill-in zone seems plausible in case of low reinforcement ratios (or for single pre-damaged filaments), but not convincing for high fibre volume content.

A different explanation is that inside the core of filament yarns a portion of filaments exists, which are weakly linked to their neighbours and thus do not significantly participate on the load transmission. In this case, the effect is independent of the reinforcement ratio but depends on the load transfer conditions in the yarn. Optical investigations on thin sections of yarns embedded in matrix by [10] support this explanation, because especially circularly shaped yarns show a large amount of voids in the cross section. However, these local investigations are not sufficient for the determination of the bond behaviour on a certain embedding length.

Regarding the ultimate capacity, it has been observed that with additional polymer-coating on the fabrics a better exploitation of the reinforcement with higher strength and ultimate strains compared to uncoated fabrics is achieved. Reasons for this effect are for instance a certain protection of the filaments in the laminating process, which might prevent outer filaments from failure. The more important reason seems to be the homogenisation of stresses in the filament yarns due to the coating, which leads to a delayed failure initiation compared to uncoated fabrics, see also [7].

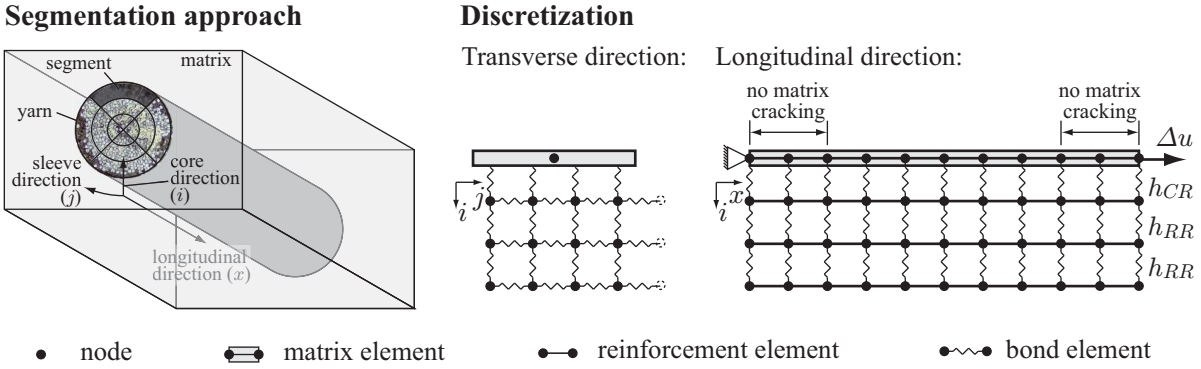

Figure 2: Segmentation of the reinforcement and schemetical discretization in the model in transverse and longitudinal direction

3 Mechanical model and numerical methods

Numerical simulations based on a reduced two-dimensional model are carried out to confirm the explanations of the load-bearing effects and mechanisms discussed above. The basic idea of the model was published earlier, see e. g. [9]. In [7], an enhanced bond law including bond degradation after reaching the bond strength is introduced. Since the model is presented in detail in the mentioned contributions, only the essential issues are described in the following.

3.1 Geometry and element types

The aim of the model is the simulation of the material and structural behaviour of TRC under uniaxial tensile loading. Neglecting influences from transverse strains due to Poisson's ratio allows for the application of basic bar elements to model the axial material properties of matrix and reinforcement, which are e. g. Young's modulus and tensile strength. In the model, bar elements representing matrix and reinforcement are arranged in longitudinal direction in series, see Figure 2. While the matrix is usually modelled with one element strand, the reinforcement is subdivided into so-called segments to take different load transfer mechanisms between the segments into account and to determine the stress distribution in the reinforcement. Thus, there are several bar element strands in parallel. The bar elements representing the matrix have a cross-sectional area of $0.0008\,\mathrm{m}^2$, see Section 2. The determination of the geometric parameters of the reinforcement segments depending on the number of yarns and their cross-sectional areas is described in [7]. In the simulations, the reinforcement is subdivided into one strand representing the fill-in zone with 36 % of the total cross-sectional area of the reinforcement and four strands representing the core of the reinforcement with 28 %, 20 %, 12 % and 4 % of the total cross-sectional area of the reinforcement. This ratio corresponds to a circular cross-section with a subdivision into five annuli with equal thickness. The cross section of a yarn is $1.1{\cdot}10^{-7}\,\mathrm{m}^2$ and the number of yarns is given with 134, which corresponds to a reinforcement ratio of about 1.9 %. The length of the bar elements is chosen with $1{\cdot}10^{-4}\,\mathrm{m}$.

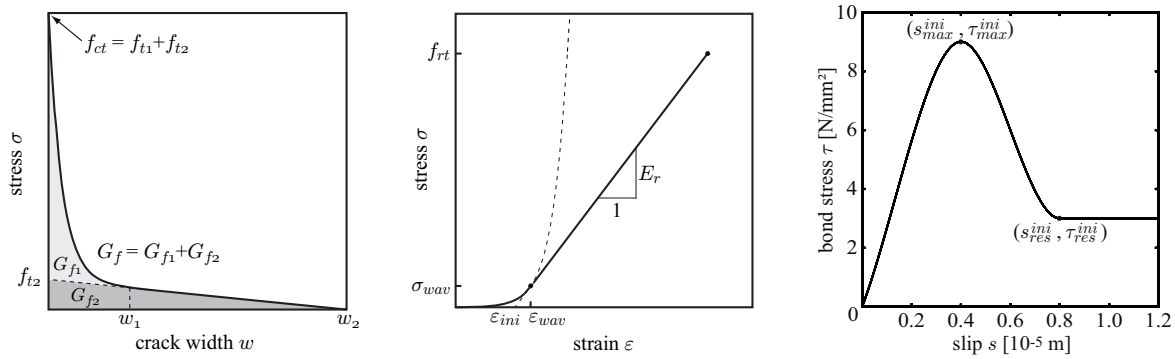

(a) Constitutive relation of matrix (tension softening)

(b) Constitutive relation of reinforcement (waviness)

(c) Bond law for matrix-reinforcement interaction

Figure 3: Constitutive relations

The bar element strands are connected at their nodes with so-called zero-thickness bond elements. The bond elements act according to bond laws, which are described in Section 3.2. According to the position of the interface, which is modelled, the bond laws may be different. It is worth to note that only the outermost reinforcement segments are directly connected to the matrix while the segments in the reinforcement core are only connected to the direct neighbours according to the scheme in Figure 2. This is also the difference to the model by [8] where also the core segments are directly connected to the matrix.

The boundary conditions of the model are given with the fixed first concrete node and the prescribed displacements at the last concrete node, see Figure 2. Furthermore, the matrix elements at both ends of the strand are not allowed to fail on lengths of 20 % of the total length to ensure an undisturbed load transmission to the reinforcement in these zones.

3.2 Constitutive relations

The constitutive behaviour of the matrix and the reinforcement can be modelled as linear-elastic up to a brittle failure. However, it is known that concrete and mortar show tension softening, which means that after reaching the tensile strength still stress can be transferred across the crack, see e. g. [2, 5, 14]. In the model, matrix tension softening is implemented according to the stress-crack width ($\sigma - w$) relation formulated by [14]

$$\sigma = f_{t1} \exp\left[-\left(\frac{w}{w_1}\right)^c\right] + f_{t2}\left(1 - \frac{w}{w_2}\right) \text{ for } 0 < w \leq w_2;\ f_{ct} = f_{t1} + f_{t2} \tag{1}$$

with the tensile strength f_{ct}, which is the sum of f_{t1} and f_{t2}, the characteristic crack widths w_1 and w_2 and the shape parameter c, see Figure 3(a). The final crack width w_2 and the tensile strength f_{ct} can be obtained from experiments, e. g. from [2]. The ratio between f_{t1} and f_{t2}, c and w_1 have to be fitted to the experimental $\sigma - w$ relation considering the fracture energy G_f. A more detailed description of the parameter determination is given in [14].

For the stress-strain ($\sigma - \varepsilon$) relation corresponding to Equation (1), w has to be related to the length of the respective bar element l_{el}, which ensures mesh-objective results as well. Since softening starts after reaching f_{ct} and ends if w_2 is reached, the $\sigma - \varepsilon$ relation is given for $f_{ct}/E_{c0} < \varepsilon < f_{ct}/E_{c0} + w_2/l_{el}$ with

$$\sigma = f_{t1} \exp\left[- \left(\frac{l_{el}\left(\varepsilon - \frac{f_{ct}}{E_{c0}}\right)}{w_1} \right)^c \right] + f_{t2} \left(1 - \frac{l_{el}\left(\varepsilon - \frac{f_{ct}}{E_{c0}}\right)}{w_2} \right) \tag{2}$$

where E_{c0} is the initial Young's modulus of the matrix. For the inelastic regime given by $f_{ct}/E_{c0} < \varepsilon < f_{ct}/E_{c0} + w_2/l_{el}$ the algorithmic stiffness is required for the Newton-Raphson iteration scheme. The instantaneous stiffness can be readily obtained as the first derivative of Equation (2) with respect to ε:

$$\frac{d\sigma}{d\varepsilon} = E_t = -\frac{c\, f_{t1}}{\left(\varepsilon - \frac{f_{ct}}{E_{c0}}\right)} \left(\frac{l_{el}\left(\varepsilon - \frac{f_{ct}}{E_{c0}}\right)}{w_1} \right)^c \exp\left[- \left(\frac{l_{el}\left(\varepsilon - \frac{f_{ct}}{E_{c0}}\right)}{w_1} \right)^c \right] - \frac{l_{el} f_{t2}}{w_2}. \tag{3}$$

In case of $\varepsilon \geq f_{ct}/E_{c0} + w_2/l_{el}$, σ and E_t are set to zero. For $\varepsilon \leq f_{ct}/E_{c0}$, the constitutive behaviour is described by Hooke's law, where E_t is equal to E_{c0}.

For the reference model, the material behaviour of the reinforcement is assumed linear elastic according to Young's modulus E_r up to brittle failure associated with σ and E_r set to zero for $\varepsilon > f_{rt}/E_r$. In order to take the initial waviness of the yarns into account, the $\sigma - \varepsilon$-relation is enhanced with an initial stress-reduced deformation, see Figure 3(b), implemented as a smooth exponential transition to the linear-elastic relation (with a positive strain shift ε_{ini}) to improve the convergence of the iteration scheme:

$$\sigma = \begin{cases} (\exp\left[a_{wav}\varepsilon\right] - 1) b_{wav} & \text{for} \quad 0 \leq \varepsilon \leq \varepsilon_{wav} \\ E_r(\varepsilon - \varepsilon_{ini}) & \text{for} \quad \varepsilon_{wav} < \varepsilon < \varepsilon_{ini} + f_{rt}/E_r \\ 0 & \text{otherwise.} \end{cases} \tag{4}$$

The factors a_{wav} and b_{wav} of the exponential function have to be determined according to the condition that the exponential function is tangent to the linear function at a pre-defined point $(\varepsilon_{wav}, \sigma_{wav})$. Again, the first derivatives are needed for the algorithmic stiffness, which are given with $d\sigma/d\varepsilon = a_{wav} b_{wav} \exp[a_{wav}\varepsilon]$ for $0 \leq \varepsilon \leq \varepsilon_{wav}$, $d\sigma/d\varepsilon = E_r$ for $\varepsilon_{wav} < \varepsilon < \varepsilon_{ini} + f_{rt}/E_r$ and $d\sigma/d\varepsilon = 0$ otherwise. The reference values of the material properties for the following simulations are given in Table 1.

In order to transfer forces between bar elements, bond elements are used, which act according to bond laws formulated as bond stress-slip ($\tau - s$) relations, see Figure 3(c). The slip s is the relative displacement between the two nodes of a bond element. The bond laws are defined by a set of i supporting points (s_i, τ_i). Between these points, it is interpolated by means of the „Piecewise Cubic Hermite Interpolating Polynomial Procedure“ (PCHIP) by [4], which preserves monotonicity and continuity in the first derivatives between consecutive intervals.

Table 1: Material properties of matrix and reinforcement; reference values

matrix				reinforcement	
E_{c0} [MN/m^2]	f_{ct} [MN/m^2]	G_f [N/m]	w_2 [m]	E_r [MN/m^2]	f_{rt} [MN/m^2]
28,500 [10]	5.0 [10]	40 [2]	$2.0{\cdot}10^{-4}$	79,950 [1]	1357 [1]

Furthermore, the bond law includes a formulation for the case of unloading based on the concept of plasticity, see [7] for more details.

Different zones of load transfer exist in a yarn due to the incomplete penetration with matrix. In the so-called fill-in zone, relatively strong adhesive bond between the matrix and the filaments occurs. This is modelled with increasing bond stresses until the bond strength τ_{max} at s_{max} is reached. Subsequently, the bond stress decreases according to the assumption of degrading bond until a value of τ_{res} at s_{res}. Afterwards, purely frictional load transfer is assumed, which is modelled with a horizontal course of the $\tau - s$-relation. The reference values for the supporting points of the bond law are given in Figure 3(c). Only the outermost reinforcement strand and the matrix strand are connected with bond elements owning this characteristic. The inner reinforcement strands are connected with bond elements with a bond law, which have bond stress values $\tau_{max} = \tau_{res} = 3\,\mathrm{N/mm^2}$ corresponding to the assumption of only frictional load transfer between the filaments.

3.3 Numerical methods

The numerical solution of the evolving equations is a non-trivial issue. Non-linearities are incorporated in both element types, which necessitate incrementally increasing loading and equilibrium iterations in every load step. Therefore, the BFGS method, see for instance [12], combined with line search is applied. In the case of cracking, which is limited to one element per load step, the system is recalculated in the cracked state at the same load level.

4 Computational results and discussion

4.1 General stress-strain behaviour

For the simulations, the reference model described in Section 3 without consideration of matrix tension softening and yarn waviness is used. In Figure 4(a), the calculated stress-strain relation is shown. As it can be seen, the characteristic stress-strain behaviour is reproduced with the model. In the cracking state, different cracking stages are well distinguishable, because stochastic variations of the tensile strength, which lead to a more continuous cracking state, are neglected in the simulations. In the final cracking state, tension stiffening can be identified as the strain gap between the stiffness of the reinforcement alone and the reference simulation. The slope of the stress-strain relation is equal to the stiffness of the reinforcement,

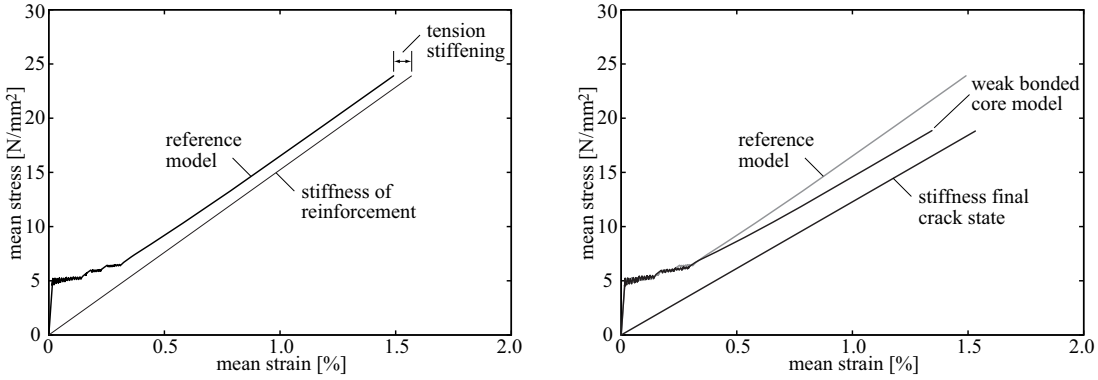

(a) Reference model (b) Weak bond in the core

Figure 4: Computed stress-strain relations for reference model and model with weak bond in the core

which means that the stiffness deficit observable in the experiments is not a simple outcome of the combination of the composite's material properties and the assumed bond characteristics.

4.2 Deficit of stiffness in the cracked state

In Section 2, two explanations for the deficit of stiffness in the final cracking state were given; the first was the assumption of simultaneous matrix cracking and filament failure in the fill-in zone. It is, of course, possible to reduce the slope of the stress-strain relation in the final cracking state if the strength of the filaments in the fill-in zone is reduced such that simultaneous matrix cracking and filament failure occurs. However, results of respective simulations published in [6] showed that the number of cracks decreased considerably compared to the case of a non-simultaneous failure. The computational results of the reference model show also that at least with the given reinforcement ratio of 1.9 % the stresses in the reinforcement are about 400 N/mm^2 and therefore far below filament tensile strength, see Figure 6. Furthermore, it was shown in [7] by means of simulations that the strength of the filaments in the fill-in zone is only reached if there is a very small amount of filaments in contact with the matrix or the bond strength between matrix and reinforcement is very large. Thus, the assumption of simultaneous matrix cracking and filament failure in the fill-in zone seems to be not sufficient to explain the reduced stiffness occurring in experimental results.

The second explanation in Section 2 was that inside the core of the yarns a portion of filaments exists, which are linked very weakly to their neighbours and are thus almost unloaded. A simulation was carried out to illustrate the effect of a weak-bonded core. Therefore, the value τ_{max} of bond law h_{RR} is reduced exponentially towards the innermost core segment starting with 3 N/mm^2 at the outermost core segment, in steps of 0.3 N/mm^2, 0.03 N/mm^2 and 0.003 N/mm^2. The resulting stress-strain relation is shown in Figure 4(b). It can be seen that the slope in the cracked state is clearly reduced compared to the reference model. Although the number of cracks is also slightly reduced, this proves the aforementioned mechanisms to be possible. A drawback is that at the ends of the specimen the concrete and the two innermost

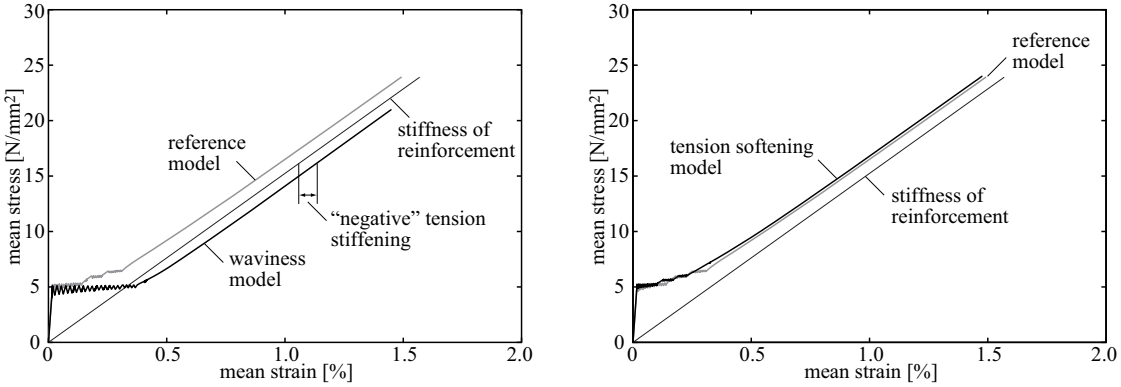

(a) Filament waviness (b) Matrix tension softening

Figure 5: Stress-strain relation in the cases of filament waviness and matrix tension softening

core segments have a slip of about 2 mm, which means that they pulled in the matrix. This is not reported by [10] and needs further investigations.

Which of both effects (premature filament failure, weak-bonded core) dominates, depends on reinforcement ratio, filament strength, yarn bundle geometry and bond properties. While the effect of unloaded filaments in the core is independent of the reinforcement ratio, it depends on the yarn shape and thus on the penetration with matrix. The effect of simultaneous matrix cracking and filament failure should be, from the theoretical point of view, especially pronounced with low reinforcement ratios and circular shaped yarns. In this case, the matrix penetrates only a small part of the yarn and the filaments in the fill-in zone are highly loaded. With low reinforcement ratios, the stress in the reinforcement is higher after matrix cracking compared to high reinforcement ratios. It is however difficult to evidence this assumption by experimental results, because with low reinforcement ratios the determination of the slope of the stress-strain relation in the final cracking state is associated with difficulties, see [10].

4.3 Waviness

Waviness of filaments, which leads to an initial stressless deformation of the filaments, influences the stress-strain behaviour of TRC. However, this effect seems to be limited to the filaments in the core of the yarn where only relatively weak bond forces occur. In the fill-in zone, an initial stressless deformation of the filaments seems to be not possible because of the strong adhesive bond between matrix and filaments, which leads to an immediate load transfer between both. Therefore, the effect of waviness should be especially noticeable with circularly shaped yarns with a large ratio of core filaments and with yarns consisting of more filaments.

A simulation is carried out to investigate the effect of waviness. The reinforcement of the reference model is modified with respect to the stiffness of the four core segments according to Equation (4). A stress-reduced deformation until a strain value $\varepsilon_{ini} = 0.3\,\%$ is introduced. The transition from the exponential function to the linear function is assumed at a stress value

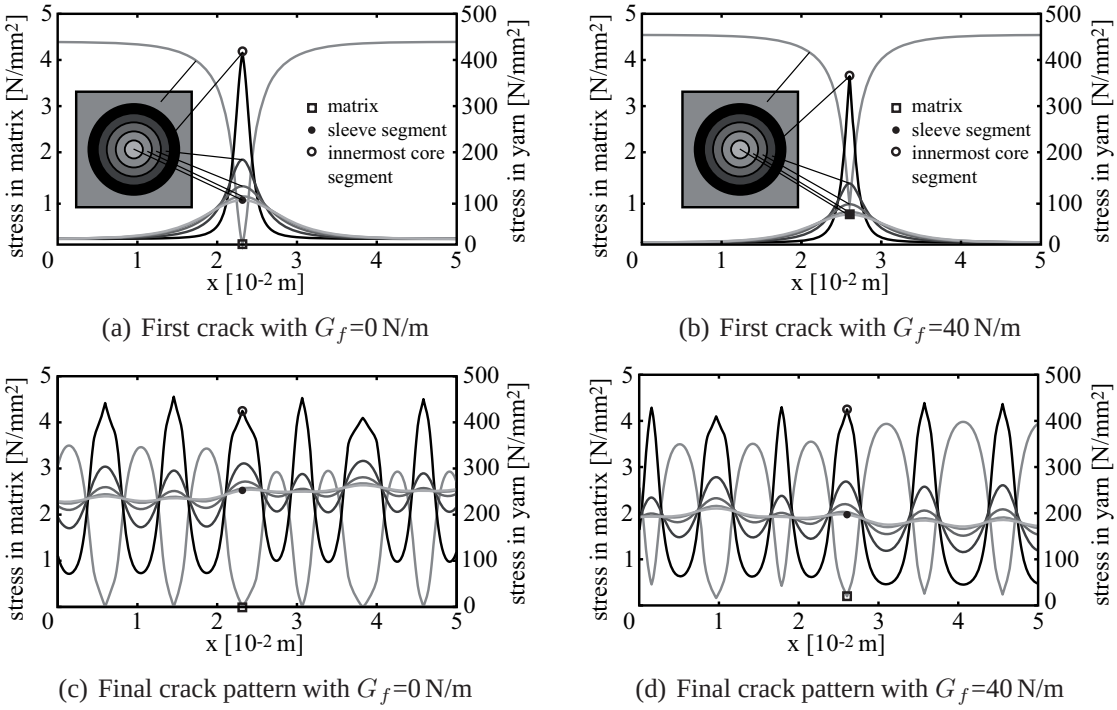

(a) First crack with G_f=0 N/m

(b) First crack with G_f=40 N/m

(c) Final crack pattern with G_f=0 N/m

(d) Final crack pattern with G_f=40 N/m

Figure 6: Normal stress distribution in matrix and reinforcement segments along the longitudinal direction in the centre part of the model

$\sigma_{wav} = 150\,\text{N/mm}^2$ with a corresponding strain $\varepsilon_{wav} = 0.488\,\%$. The parameters of the exponential function were determined with $a_{wav} \approx 482$ and $b_{wav} \approx 16$.

In the stress-strain relation, see Figure 5(a), the cracking state is extended to a larger strain range compared to the reference case, which also leads to „negative“ tension stiffening. Contrary to the reference model, stress levels at which cracks occur are almost constant. The number of cracks and the slope in the final cracking state are however not influenced. The ultimate strain is almost on the same level as in the reference model, while the ultimate stress decreases with waviness. This can be explained with the stress concentration in the fill-in zone reaching the tensile strength earlier due to the delayed activation of the reinforcement core.

4.4 Matrix tension softening

The contribution of the matrix to crack-bridging due to tension softening reduces stresses in the reinforcement right after matrix cracking. For the following simulation, the reference model is enhanced with matrix tension softening according to Equations (2) and (3). Respective parameters were determined with $f_{t1} = 4.9\,\text{N/mm}^2$, $f_{t2} = 0.1\,\text{N/mm}^2$, $c = 1$ and $w_1 = 6.12{\cdot}10^{-6}\,\text{m}$ with a good agreement to the $\sigma - w$-relation by [2] for matrix PZ-0899-01.

In Figure 5(b), the simulated stress-strain relations of the reference model and the model considering matrix tension softening are shown. It can be seen that the cracking state is shorter in

case of matrix tension softening, although the number of cracks is identical. Furthermore, the stress drops after matrix cracks are smaller in case of matrix tension softening. The stiffness in the cracked state is only influenced by matrix tension softening right after reaching the final cracking state. With further increased loading and opening cracks, it merges towards the stiffness of the reference case.

The post-cracking resistance of the matrix leads to reduced stress in the reinforcement after matrix cracking. This can be seen in Figure 6 where the stress distributions along the longitudinal direction x in the centre part of the model on a length of 0.05 m are compared for the reference model and the model with matrix tension softening. At the first crack, it is observable that in case considering matrix fracture energy, the matrix is still loaded with a stress of about 1 N/mm^2. Correspondingly, the stress in the outermost reinforcement strand decreases to about 350 N/mm^2 compared to about 400 N/mm^2 in the reference model and a matrix stress of 0 N/mm^2. In the final cracking state, see Figure 6(d), some stress can also be transferred across the matrix and, thus, the stresses in the reinforcement are lower for the case with matrix tension softening. This confirms the expectation discussed in Section 4.2 that premature filament failure might not be the only cause for the stiffness deficit after multiple cracking especially in case of high reinforcement ratios.

5 Conclusions

Textile Reinforced Concrete shows a complex material behaviour, which arises from the nonlinear material behaviour of its constituents, the matrix and the reinforcement, and the nonlinear load transfer mechanisms in between. In this paper, a number of characteristic effects concerning the constitutive behaviour of TRC were addressed and analysed by means of numerical simulations with a reduced two-dimensional model.

The effect of deficit of stiffness in the final cracking state was discussed controversially. It was pointed out that premature filament failure might be not the only cause for this effect. Weakly bonded core filaments lead to a similar effect. Furthermore, it was confirmed that waviness of filaments and yarns could lead to a „negative“ tension stiffening effect, while tension softening of the matrix with its currently low fracture energy has only minor influence on the material behaviour of TRC. However, further investigations with short-fibre enhanced matrices, which may even show strain-hardening behaviour, might be interesting.

6 Acknowledgements

The authors gratefully acknowledge the financial support of this research from Deutsche Forschungsgemeinschaft DFG (German Research Foundation) within the Sonderforschungsbereich 528 (Collaborative Research Center) „Textile Reinforcement for Structural Strengthening and Retrofitting“ at Technische Universität Dresden.

7 References

[1] ABDKADER, A.: *Charakterisierung und Modellierung der Eigenschaften von AR-Glasfilamentgarnen für die Betonbewehrung*. TU Dresden : Dresden, 2004 – PhD thesis

[2] BROCKMANN, T.: *Mechanical and fracture mechanical properties of fine grained concrete for textile reinforced composites*. RWTH Aachen : Aachen, 2006 – PhD thesis

[3] BRUCKERMANN, O.: *Zur Modellierung des Zugtragverhaltens von textilbewehrtem Beton*. RWTH Aachen : Aachen, 2007 – PhD thesis

[4] FRITSCH, F.N.; CARLSON, R.E.: Monotone piecewise cubic interpolation. *SIAM Journal on Numerical Analysis* 17(2) (1980), p. 238–246

[5] GOPALARATNAM, V.S.; SHAH, S.P.: Softening response of plain concrete in direct tension. *ACI Journal* 28(3) (1985), p. 310–323

[6] HARTIG, J.; HÄUSSLER-COMBE, U.; SCHICKTANZ, K.: Modelling the uniaxial load-bearing behaviour of textile reinforced concrete with a lattice approach including damage. In: TRIANTAFILLOU, T., (Ed.): *FRPRCS-8, 16-18, July, 2007, Patras, Greece*, University of Patras : Patras, 2007, no. 17-2 (CD of full papers)

[7] HARTIG, J.; HÄUSSLER-COMBE, U.; SCHICKTANZ, K.: Influence of bond properties on the tensile behaviour of textile reinforced concrete. *Cement & Concrete Composites*, 30(10) (2008), p. 898–906

[8] HEGGER, J.; WILL; N., BRUCKERMANN, O.; VOSS, S.: Load-bearing behaviour and simulation of textile reinforced concrete. *Materials & Structures*, 39 (2006), p. 765–776

[9] HÄUSSLER-COMBE, U.; HARTIG, J.: Bond and failure mechanisms of textile reinforced concrete (TRC) under uniaxial tensile loading. *Cement & Concrete Composites*, 29(4) (2007), p. 279–289

[10] JESSE, F.: *Load Bearing Behaviour of Filament Yarns in a Cementitious Matrix (in German)*. TU Dresden : Dresden, 2004 – PhD thesis

[11] LEPENIES, I.G.: *Zur hierarchischen und simultanen Multi-Skalen-Analyse von Textilbeton*. TU Dresden : Dresden, 2007 – PhD thesis

[12] MATTHIES, H.; STRANG, G.: The solution of non-linear finite element equations. *International Journal for Numerical Methods in Engineering*, 14 (1979), p. 1613–1626

[13] MOLTER, M.: *Zum Tragverhalten von textilbewehrtem Beton*. RWTH Aachen : Aachen, 2005 – PhD thesis

[14] REMMEL, G.: *Zum Zug- und Schubtragverhalten von Bauteilen aus hochfestem Beton (DAfStb Heft 444)*. Beuth : Berlin, 1994.

[15] RICHTER, M.: *Entwicklung mechanischer Modelle zur analytischen Beschreibung der Materialeigenschaften von textilbewehrtem Feinbeton*. TU Dresden : Dresden, 2005 – PhD thesis